



Sediments as a Source of Iron, Manganese, Cobalt and Nickel to Continental Shelf Waters (Louisiana, Gulf of Mexico)

Wytze K. Lenstra^{1*}, Niels A. G. M. van Helmond¹, Olga M. Żygadłowska¹, Roosmarijn van Zummeren¹, Rob Witbaard² and Caroline P. Slomp¹

¹ Department of Earth Sciences—Geochemistry, Utrecht University, Utrecht, Netherlands, ² Department of Estuarine and Delta Systems, NIOZ, Netherlands Institute for Sea Research, Utrecht University, Utrecht, Netherlands

OPEN ACCESS

Edited by:

Sunil Kumar Singh,
Physical Research Laboratory, India

Reviewed by:

Martha Gledhill,
Helmholtz Association of German
Research Centres (HZ), Germany
Juan Santos Echeandia,
Spanish Institute of Oceanography
(IEO), Spain

*Correspondence:

Wytze K. Lenstra
w.k.lenstra@uu.nl

Specialty section:

This article was submitted to
Marine Biogeochemistry,
a section of the journal
Frontiers in Marine Science

Received: 09 November 2021

Accepted: 07 January 2022

Published: 27 January 2022

Citation:

Lenstra WK, van Helmond NAGM, Żygadłowska OM, van Zummeren R, Witbaard R and Slomp CP (2022) Sediments as a Source of Iron, Manganese, Cobalt and Nickel to Continental Shelf Waters (Louisiana, Gulf of Mexico). *Front. Mar. Sci.* 9:811953. doi: 10.3389/fmars.2022.811953

Continental shelf sediments are a key source of trace metals to the ocean. In this study, we investigate the impact of sedimentary processes on water column concentrations of iron (Fe), manganese (Mn), cobalt (Co), and nickel (Ni) at five stations on the Louisiana continental shelf and slope, Gulf of Mexico. The highest trace metal concentrations were observed close to the seafloor at the most nearshore shelf station (water depth of 16 m), with most of the metals present in particulate form. This enrichment in the bottom water is likely the combined effect of input of trace metals in suspended matter from the Mississippi/Atchafalaya Rivers and, for Mn, Co, and Ni, benthic release from the shelf sediments. While particulate matter was the dominant carrier of Fe and Mn in bottom waters in the shelf and slope regions, Co and Ni were nearly exclusively present in dissolved form. Hence, lateral transport of Co and Ni in shelf waters is decoupled from that of Fe and Mn. Concentrations of particulate and dissolved trace metals in the water column generally decreased from the shelf to the slope, while those in the sediment increased. This suggests an increased retention of metals deposited on the sediment with distance from the coast, linked to the decrease in organic matter input and associated reductive sediment processes. The offshore decline in sediment trace metal mobilization is likely typical for river-dominated continental margins where most organic matter is deposited close to the coast.

Keywords: bio-essential, benthic flux, organic matter, trace metals, lateral transport, GEOTRACES

1. INTRODUCTION

Continental shelf sediments are a key source of bio-essential trace metals, such as iron (Fe), manganese (Mn), cobalt (Co), and nickel (Ni), to ocean waters (Lam and Bishop, 2008; Lam et al., 2012; Noble et al., 2017). High benthic release of trace metals is expected on river-dominated margins because of the continuous supply of particulate material (Meybeck, 2003; Severmann et al., 2010; Lenstra et al., 2019). Transport of trace metals from the coastal zone to the open ocean typically involves one or more cycles of benthic release, lateral transport in the water column and redeposition in particulate form (Raiswell and Canfield, 2012). Further insight in this recycling is essential for our understanding of present-day trace metal fluxes from the coastal to the open ocean and how these fluxes may change in the future (Henderson et al., 2018).

In shelf sediments, dissolved Fe and Mn is produced through reductive dissolution of Fe and Mn oxy(hydr)oxides (henceforth termed Fe and Mn oxides), driven by degradation of organic matter and/or the associated production of reductants such as sulfide (Burdige, 2006). Dissolved Co and Ni can be released in parallel with Fe and Mn, either from Fe and Mn oxides upon their reduction or from organic matter upon its degradation (Goldberg, 1954; Tribovillard et al., 2006). The dissolved Fe and Mn can then diffuse upwards and form Fe and Mn oxides when surface sediments are oxic (Santos-Echeandia et al., 2009; McManus et al., 2012; Dale et al., 2015). The Fe and Mn oxides, in turn, can scavenge dissolved Co and Ni (Moffett and Ho, 1996; Peacock and Sherman, 2007).

Some dissolved Fe, Mn, Co, and Ni may escape to the overlying water, however, even when bottom waters are oxic. This occurs, for example, when the oxic surface layer of the sediment is very thin and the kinetics of oxidation of dissolved metals in the porewater are not fast enough to allow for formation of metal oxides in the sediment (Slomp et al., 1997; Severmann et al., 2010; Klar et al., 2017). Bioirrigation by macrofauna can lead to bypassing of the oxic surface sediment by creating a direct transport pathway between porewaters at depth in the sediment and overlying waters (Thamdrup et al., 1994; Lenstra et al., 2019). Benthic release of metals is also modulated by the availability of sulfide in porewaters because Fe, Mn, Co, and Ni can be retained in authigenic sulfide minerals (Huerta-Diaz and Morse, 1992; Tribovillard et al., 2006; Large et al., 2014). In particular, the availability of reactive Fe oxides versus sulfide produced through sulfate reduction can play a critical role in determining the benthic release of metals (Lenstra et al., 2021a). In summary, multiple factors control the benthic release of Fe, Mn, Co, and Ni, including bottom water oxygen, oxygen penetration depth in the sediment, the input and reactivity of the incoming organic matter, macrofaunal activity and the rate of sulfide production in the sediment (Sundby et al., 1986; McManus et al., 2012; Scholz et al., 2014; Lenstra et al., 2019).

Trace metals in shelf and slope waters can be transported offshore with currents and may undergo repeated cycles of deposition and remobilization (Raiswell and Canfield, 2012; Morton et al., 2019). While larger particles are expected to sink and settle rapidly at the seafloor, smaller particles, and dissolved species can be transported over large distances with only limited deposition (Jeandel et al., 2015). In oxic waters, dissolved Fe(II) and Mn(II) or Mn(III) can oxidize as particulate Fe and Mn oxides. If these oxides then scavenge dissolved Co and Ni, the water column transport of these trace metals will be coupled to that of Fe and Mn (Little et al., 2015; Vance et al., 2016). However, when organic ligands are present, dissolved Fe, Mn, Co, and Ni can also remain in solution through organic complexation (e.g., Gledhill and van den Berg, 1994; Oldham et al., 2017). We currently do not know which of these mechanisms is dominant, how this affects the distribution and transport of particulate and dissolved trace metals in the water column and what role remobilization of (trace) metals from shelf sediments plays during this lateral transport.

In this study, we assess the potential role of sediment processes in determining the distribution of particulate and dissolved Fe,

Mn, Co, and Ni in the water column at five stations along an offshore transect on the Louisiana continental shelf and slope. The shelf is strongly influenced by discharge of the Mississippi/Atchafalaya Rivers and is subject to seasonal bottom water hypoxia (oxygen concentrations $<63 \mu\text{mol L}^{-1}$; Rabalais et al., 2002). Besides water column analyses of Fe, Mn, Co, and Ni, we present the speciation of Fe in the suspended matter and sediment, porewater profiles of Fe and Mn, sediment depth profiles of Fe, Mn, Co, and Ni and *in-situ* benthic fluxes of the same metals for the most nearshore stations. We observe a distinct offshore decline in trace metal concentrations in the water column, with particulate matter dominating the transport of Fe and Mn near the seafloor while Co and Ni are mostly present in dissolved form.

2. METHODS

2.1. Study Area and Sampling

Our study area is located along a water depth transect on the Louisiana continental shelf and slope in the northern Gulf of Mexico (Figure 1). The coastal zone in this region is strongly influenced by freshwater and nutrient inputs from the Mississippi/Atchafalaya Rivers (Rabalais et al., 2002; Fennel and Testa, 2019). A large part of the continental shelf, on average approximately $14,000 \text{ km}^2$ for the period 1985–2020, is seasonally hypoxic (Turner and Rabalais, 2019; Pitcher et al., 2021). The hypoxia is mostly observed in water depths of 5 to 30 m and results from the combination of fresh-water-induced stratification and local high primary production (Fennel and Testa, 2019). Sediment oxygen uptake accounts for ca. 30% of total oxygen uptake below the pycnocline and hence is critical for hypoxia generation on the shelf (Fennel and Testa, 2019). Suspended matter and solutes derived from the Louisiana continental shelf and slope are transported to the open ocean by

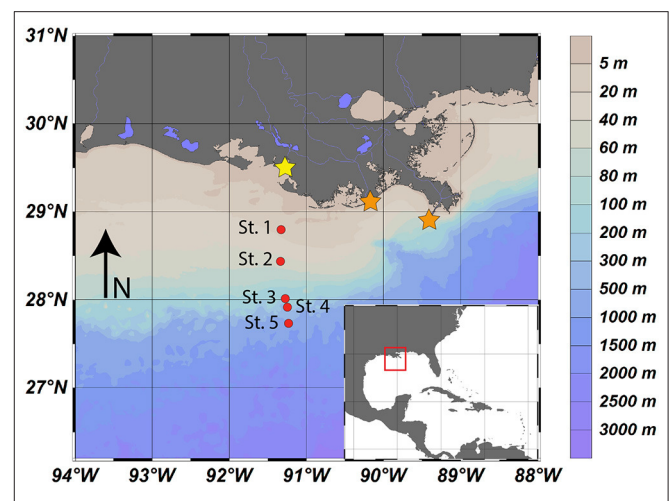


FIGURE 1 | Locations of the five stations sampled on the Louisiana continental shelf and slope, Gulf of Mexico in March 2018. Stars indicate the main river mouths of the Atchafalaya River (yellow) and Mississippi River (orange). This figure was made with Ocean Data View (Schlitzer, 2015).

the Loop Current, which variably interacts with the continental shelf (Charette et al., 2016; Mellett and Buck, 2020).

Sediment and water column samples were collected during a cruise with *R/V Pelagia* in March 2018. A total of five stations were sampled, of which two on the continental shelf and three on the continental slope. Of the two continental shelf stations one station (station 1) is located in an area of the shelf that is regularly affected by hypoxia (Pitcher et al., 2021). Water column depth profiles of temperature, salinity, density, and beam transmission and dissolved oxygen were obtained with a CTD profiler equipped with an oxygen sensor (SBE43). No oxygen sensor measurements are available for stations 3 and 4. Water samples at stations 1, 3, and 4 were collected with a regular CTD. At stations 2 and 5, water samples were collected using a TITAN-CTD frame, with 24 ultraclean sampling bottles of 24 L made of polyvinylidene fluoride and titanium (Rijkenberg et al., 2015). The use of the regular CTD system might have led to slightly higher concentrations of dissolved trace metal concentrations, especially at stations 3 and 4. After deployment the ultraclean CTD system was moved to a Class-100 container for subsampling. At all stations, unfiltered samples for total dissolvable Fe, Mn, Co, and Ni (henceforth termed TdFe, TdMn, TdCo, and TdNi) were taken from the samplers using acid-washed LDPE tubing. Samples for dissolved Fe, Mn, Co, and Ni were obtained using a 0.2 μm Sartobran 300 cartridge (Sartorius), which was rinsed with 0.5 L of the sample prior to final collection into the sample bottle. Samples were collected in acid-washed 60 mL LDPE bottles (Nalgene). Samples were acidified to pH 1.8 by adding 120 μL of distilled (i.e., ultrapure) 10 M HCl to 60 mL of sample. Samples were stored at 4°C and brought to room temperature before analysis. Sensor measurements and water samples that were taken closest to the seafloor were assumed to reflect the composition of bottom waters. *In-situ* pumping to collect suspended matter was performed for 1–4 h near the sea surface and near the seafloor at stations 1, 2, 3, and 5 using two McLane pumps (1x WTS-LV, 1x WTS-LV Dual Filter). After retrieval of the pumps, residual water in the filter heads was removed by vacuum pumping and the filters (Supor, 0.8 μm , 142 mm diameter) were placed in petri-dishes, sealed in plastic bags and stored at –20°C.

Sediment cores at all stations were collected with an Oktopus multi-corer (inner diameter: 10 cm) using polycarbonate tubes. Only sediments with a minimum of ca. 10 cm overlying water and an intact sediment surface were processed further. At all stations, two bottom water samples were taken directly after core retrieval. Sediment cores were sectioned at intervals of 0.5 to 3 cm under a nitrogen atmosphere into 50 mL centrifuge tubes at 18°C. The centrifuge tubes were centrifuged on board at 4,500 rpm for 25 min to extract porewater. Subsequently, the remaining sediment was stored under a nitrogen atmosphere at –20°C for solid phase analyses onshore. A second core was sliced into pre-weighed glass vials at the same depth resolution and stored at –20°C upon the determination of water content and ^{210}Pb analysis.

Porewater and bottom water was filtered through disposable nylon syringe 0.45 μm pore size filters and subsampled under a nitrogen atmosphere. A 0.5 mL subsample for sulfide analysis was immediately transferred into a glass vial containing 2 mL 2%

zinc acetate. A subsample of 0.15 mL was transferred to a 2 mL glass vial for sulfate (SO_4^{2-}) analysis. Subsamples for dissolved Fe, Mn, Co, and Ni were acidified with 10 μL 10 M suprapur HCl per mL of sample. Aliquots of the remaining porewater were used to measure ammonium (NH_4^+), nitrate (NO_3^-), and nitrite (NO_2^-). All subsamples were stored at 4°C. *In-situ* benthic flux measurements were carried out at station 1 and 2 with an Albex lander (Witbaard et al., 2000). The sediment from all three chambers per lander was sieved over a 0.5 mm mesh size to collect macrofauna. These macrofauna samples were stored in 4% formaldehyde in plastic jars (Eleftheriou and McIntyre, 2007) until determination and quantification.

2.2. Water Column Analyses

The concentration of Fe in water column samples was determined by flow injection chemiluminescence with pre-concentration detection (Klunder et al., 2011). Total dissolvable Fe concentrations were determined 3 months after sample collection. All samples per station were analyzed in triplicate in the same run. The blank of acidified ultrapure water (pH = 1.8) was $32 \pm 39 \text{ pmol L}^{-1}$ ($n = 194$). The average limit of detection (LOD), calculated as the standard deviation of the analysis of oligotrophic seawater with known trace metal concentrations, multiplied by 3, was $86 \pm 120 \text{ pmol L}^{-1}$ ($n = 19$). The accuracy of the system was checked daily using GEOTRACES reference seawater. For the inhouse reference material (SLEW-3), we measured an average value of $4.11 \pm 0.036 \text{ nmol L}^{-1}$, consistent with the community reference value of $4.09 \pm 0.017 \text{ nmol L}^{-1}$. The concentrations of Co, Mn, and Ni were determined by Inductively Coupled Plasma Mass Spectrometry (ICP-MS; Nexion ICP-MS (Perkin Elmer)) after pre-concentration with an SC-DX SeaFAST S2 (Elemental Scientific). Total dissolvable Co, Mn, and Ni were determined 7 months after sample collection. The LOD values for Co, Mn, and Ni were 0.027 ± 0.004 , 0.11 ± 0.024 , and $0.99 \pm 0.12 \text{ nmol L}^{-1}$ ($n=5$), respectively, and the values of the oligotrophic seawater were 0.77 ± 0.9 , 0.9 ± 0.5 , and $4.41 \pm 0.52 \text{ nmol L}^{-1}$ ($n=40$), respectively. For the reference material SLEW-3, values for Co, Mn and Ni of 2.56 ± 0.99 , 29.01 ± 2.21 , and $21.29 \pm 1.99 \text{ nmol L}^{-1}$ ($n=12$), respectively, were obtained, consistent with the community reference values of 1.5 ± 0.36 , 27.79 ± 3.80 , and $20.96 \pm 1.19 \text{ nmol L}^{-1}$, respectively. Further details on the Fe, Co, Mn, and Ni analyses are given in **Appendix Section 1.1**.

Iron and Mn in suspended matter were determined on a quarter of each Supor filter using a 4-step sequential extraction procedure (**Supplementary Table 3**; based on Claff et al., 2010; Raiswell et al., 2010; Lenstra et al., 2021b). After extraction, all solutions were filtered through 0.45 μm pore size filters prior to analysis. Total Fe in the extraction solutions was determined colorimetrically using the 1, 10-phenanthroline method (Federation, Water Environmental). Both Fe(II) and total Fe were measured in the 1 M HCl solution and Fe(III) was calculated by subtracting the Fe(II) pool from total Fe. The values of the blanks (i.e., filters without sample) for Fe determination were $0.19 \pm 0.39 \text{ nmol L}^{-1}$ ($n = 15$). Total Mn in the extraction solutions was determined colorimetrically using

the formaldoxime method (Brewer and Spencer, 1971) but was always below the detection limit ($1 \mu\text{mol L}^{-1}$).

2.3. Porewater Analyses and *in-situ* Benthic Fluxes

Porewater samples for NH_4^+ , NO_3^- , and NO_2^- were analyzed on board with Quattro gas-segmented continuous flow analysers using the indophenolblue method (NH_4^+ ; Koroleff, 1969) and the sulphanyl-amide method (NO_3^- and NO_2^- ; Grasshoff and Ehrhardt, 1983). Porewater sulfide was determined spectrophotometrically using phenylenediamine and ferric chloride (Cline, 1969). Porewater samples for SO_4^{2-} were analyzed by ion-chromatography. Dissolved Fe and Mn were analyzed by Inductively Coupled Plasma Optical Emission Spectroscopy (ICP-OES; Spectro Arcos). Dissolved Co and Ni were analyzed by ICP-MS. Porewater concentrations were around or below the detection limit (0.5 and $0.8 \mu\text{mol L}^{-1}$, respectively) and are therefore not presented.

Diffusive fluxes of dissolved Fe and Mn ($\text{mmol m}^{-2} \text{d}^{-1}$) across the sediment-water interface were calculated using Fick's first law of diffusion taking into account porosity, ambient salinity, pressure, and temperature at each station using the R package: *marelac* (Soetaert et al., 2010). *In-situ* fluxes of oxygen, DIC, Fe, Mn, Co, and Ni across the sediment-water interface were determined with a benthic lander, equipped with three chambers made of the inert plastic delron. A detailed description of the benthic lander and sample analysis is given in Appendix Section 1.2.

2.4. Solid Phase Analyses

All sediments were freeze-dried and the porosity was determined from the weight loss upon freeze drying. Freeze-dried sediments were ground and homogenized using an agate mortar and pestle inside an argon-filled glovebox and subsequently separated into a fraction that was stored under oxic conditions (oxic fraction) and a fraction that was stored under an argon atmosphere (anoxic fraction). Speciation of solid phase Fe and sulfur (S) was determined on the anoxic subsamples to avoid oxidation artifacts (Kraal et al., 2009). All other analyses were performed on the oxic subsamples.

To determine the total elemental concentrations of aluminum (Al), Co, Fe, Mn, Ni, and S, ca. 125 mg of sediment was digested in 2.5 ml mixed acid ($\text{HNO}_3\text{:HClO}_4$; 2:3) and 2.5 ml 40% HF at 90°C . After fuming off the acids, the residue was redissolved in 4.5% HNO_3 . The solutions were subsequently analyzed on an ICP-OES. The analytical uncertainty based on duplicates and triplicates was <1% for Al, <4.2% for Co, <1.6% for Fe, <2.5% for Mn, <2.3% for Ni, and <1.7% for S. A second subsample of circa 300 mg was decalcified with 2 wash steps of 1M HCl (Van Santvoort et al., 2002) and subsequently dried, powdered and analyzed for carbon (C) using an elemental analyser (Fisons Instruments model NA 1500 NCS). Organic C content was determined after correction for the weight loss following decalcification. The analytical uncertainty based on duplicates and triplicates was <0.07 wt%. An anoxic subsample of ca. 50 mg was subjected to steps 1 to 5 of the sequential extraction procedure for Fe (Supplementary Table 3).

Average analytical uncertainty, based on duplicates, was <7.5% for all fractions. A second anoxic subsample of ca. 500 mg was subjected to a sequential S-extraction according to Burton et al. (2008) (Supplementary Table 3). Acid Volatile Sulfur (AVS) and Chromium Reducible Sulfur (CRS) were determined by iodometric titration of the alkaline Zn-acetate trap (Federation, Water Environmental). The average analytical uncertainty based on duplicates was <1.5 $\mu\text{mol g}^{-1}$ for AVS and CRS. All solid phase measurements were salt corrected based on porosity and *in-situ* bottom water salinity (Table 1). Sediment accumulation rates at all five stations were determined from depth profiles of ^{210}Pb . A detailed description of the ^{210}Pb analysis and determination of sediment accumulation rates is given in Appendix Section 1.3.

3. RESULTS

3.1. General Water Column Characteristics

Vertical profiles of salinity, temperature, and density indicate a stratified water column at all stations (Figure 2). Bottom water salinity ranged from 35 to 36.6 (Table 1). Bottom water temperature decreased from 21.4°C at station 1 to 7.8°C at station 5 (Table 1). A distinct offshore increase in the beam transmission, which is inversely correlated with the concentration of suspended particles (e.g., Wells and Kim, 1991), was observed for the bottom water (Figure 2D). Only the bottom water oxygen concentration at station 1 was in the hypoxic range (i.e., $56 \mu\text{mol L}^{-1}$; Table 2).

3.2. Water Column Fe, Mn, Co, and Ni

Water column concentrations of total dissolvable and dissolved Fe, Mn, Co, and Ni were highest at station 1 and decreased offshore toward station 5, with, for Co and Ni some variation at stations 3 and 4 that might be related to the use of a regular instead of the ultraclean CTD (Figures 3, 4). The offshore decline is particularly apparent when comparing total dissolvable metals in bottom waters at station 1 and 5: here, we observe a decrease from 15800 to 4.5 nmol L^{-1} for TdFe, from 926 to 2.8 nmol L^{-1} for TdMn, from 8.5 to 0.2 nmol L^{-1} for TdCo and from 24.7 to 4.4 nmol L^{-1} for TdNi (Figures 3, 4). In some cases, trace metal concentrations were elevated close to the sea surface, for example as observed for total and dissolved Mn, Co, and Ni at station 2

TABLE 1 | Coordinates, water depth, bottom water salinity, and temperature at the 5 stations sampled on the Louisiana continental shelf and slope.

station	location	Latitude	Longitude	Water depth mbss	Salinity	Temperature °C
		N	W			
St. 1	Shelf	28°48.546'	91°20.116'	16	35.6	21.4
St. 2	Shelf	28°26.621'	91°20.235'	53	36.4	20.4
St. 3	Slope	28°0.400'	91°16.380'	130	36.6	20.2
St. 4	Slope	27°54.535'	91°15.554'	288	35.7	13.5
St. 5	Slope	27°44.216'	91°13.515'	546	35.0	7.8

Unit mbss is meters below sea surface.

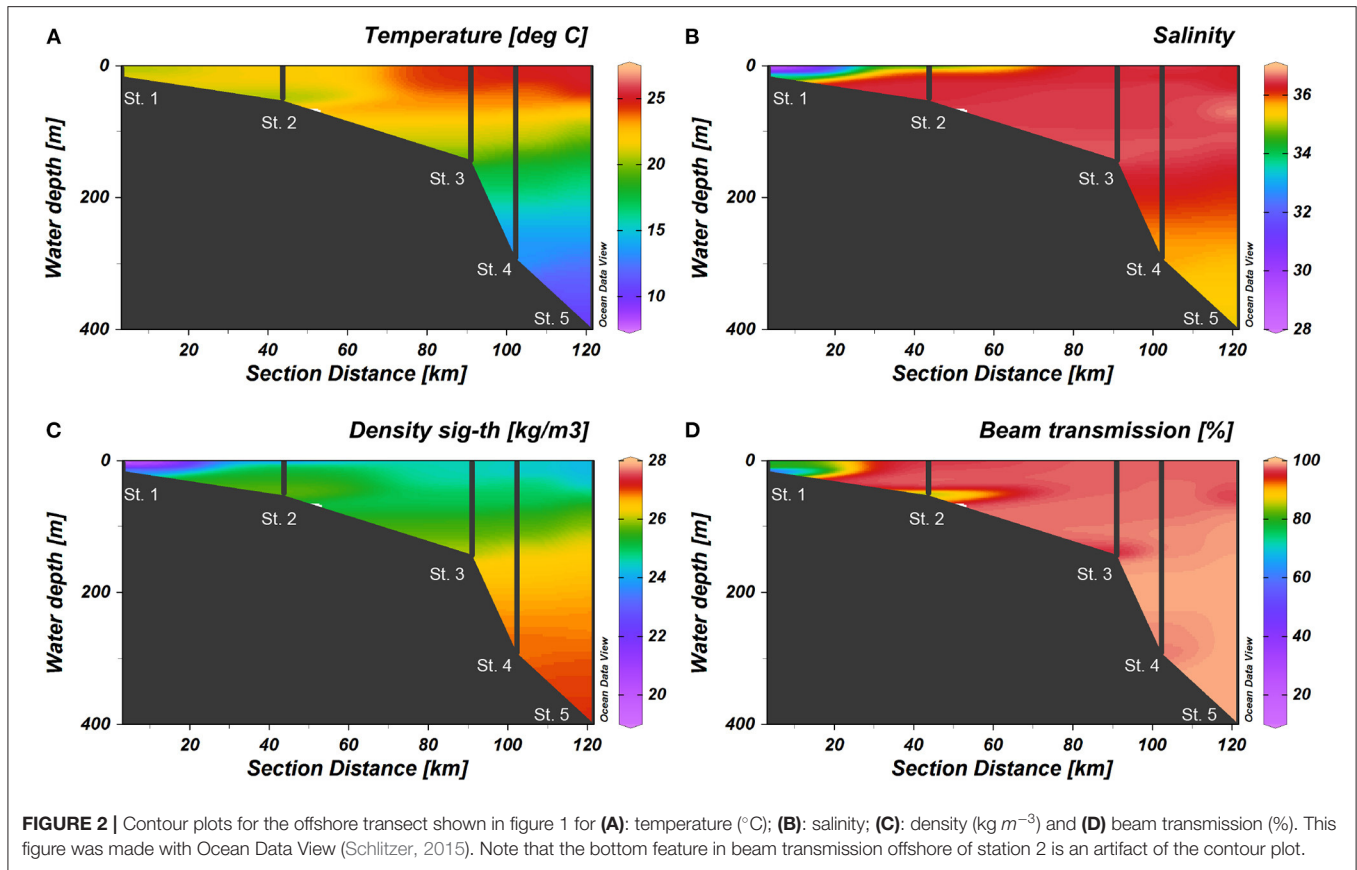


TABLE 2 | Key station characteristics: bottom water oxygen (O_2) is the average oxygen concentration at the start of the *in-situ* benthic chamber incubations (stations 1 and 2) or from the CTD (station 5).

station	O_2 Bottom water $\mu\text{mol L}^{-1}$	O_2 uptake $\text{mmol m}^{-2} \text{d}^{-1}$	NO_3^- penetration depth cm	Sed. rate cm yr^{-1}	Organic C wt %	Carbon oxidation rate $\text{mmol m}^{-2} \text{d}^{-1}$	Macrofaunal density ind. m^{-2}
St. 1	56.2±2.8	17.3±0.76	1.75	1.6	0.83	50	141±20
St. 2	184±0.03	26.1±10.5	0.25	1.5	1.10	30	49±25
St. 3	n.a.	n.a.	1.75	0.2	0.54	n.a.	n.a.
St. 4	n.a.	n.a.	2.75	0.15	1.33	n.a.	n.a.
St. 5	119.2	n.a.	7.5	0.27	1.19	n.a.	n.a.

O_2 uptake is calculated from the change in O_2 concentrations in lander boxes (Supplementary Figure 1). NO_3^- penetration depth (Supplementary Figure 4). Sedimentation rate based on ^{210}Pb depth profiles (Supplementary Figure 2). Organic carbon content in the surface sediment (0–0.5 cm). Carbon oxidation rate is based on the *in-situ* measured benthic flux of DIC. Macrofaunal density (individuals m^{-2}), species specific data per chamber are available in Supplementary Tables 1 and 2. n.a. is not available.

(Figure 3). The lowest concentrations of dissolved Fe, Mn, Co, and Ni in the water column were observed at station 5 (average of 0.65, 0.95, 0.14, 3.3 nmol L^{-1} , respectively).

Dissolved Fe accounted for only a small percentage of TdFe at station 1 but this increased with distance from the coast to station 5 (0.3 to 40%, respectively; Figure 4B). Dissolved Mn accounted for an appreciable to major fraction of the TdMn pool, accounting for 23 to 80%. Dissolved Co and Ni almost solely accounted for the TdCo and TdNi pool, except at station 1 where particulate Co and Ni were also present (Figures 4A,B).

Suspended matter collected from the bottom water was enriched in Fe when compared to surface waters at the two shelf

stations (Table 3). For suspended matter samples, on average 13% of the total Fe was extracted by ascorbic acid with the remainder of the reactive Fe being distributed in varying amounts over the other phases. Concentrations of Mn in the suspended matter samples were below detection.

3.3. Sediment and Porewater Geochemistry and Benthic Release

Sedimentation rates were much higher at the stations on the shelf (1.5 and 1.6 cm yr^{-1}) than at those located on the slope (0.15–0.27 cm yr^{-1} ; Supplementary Figure 2 and Table 2). Organic carbon

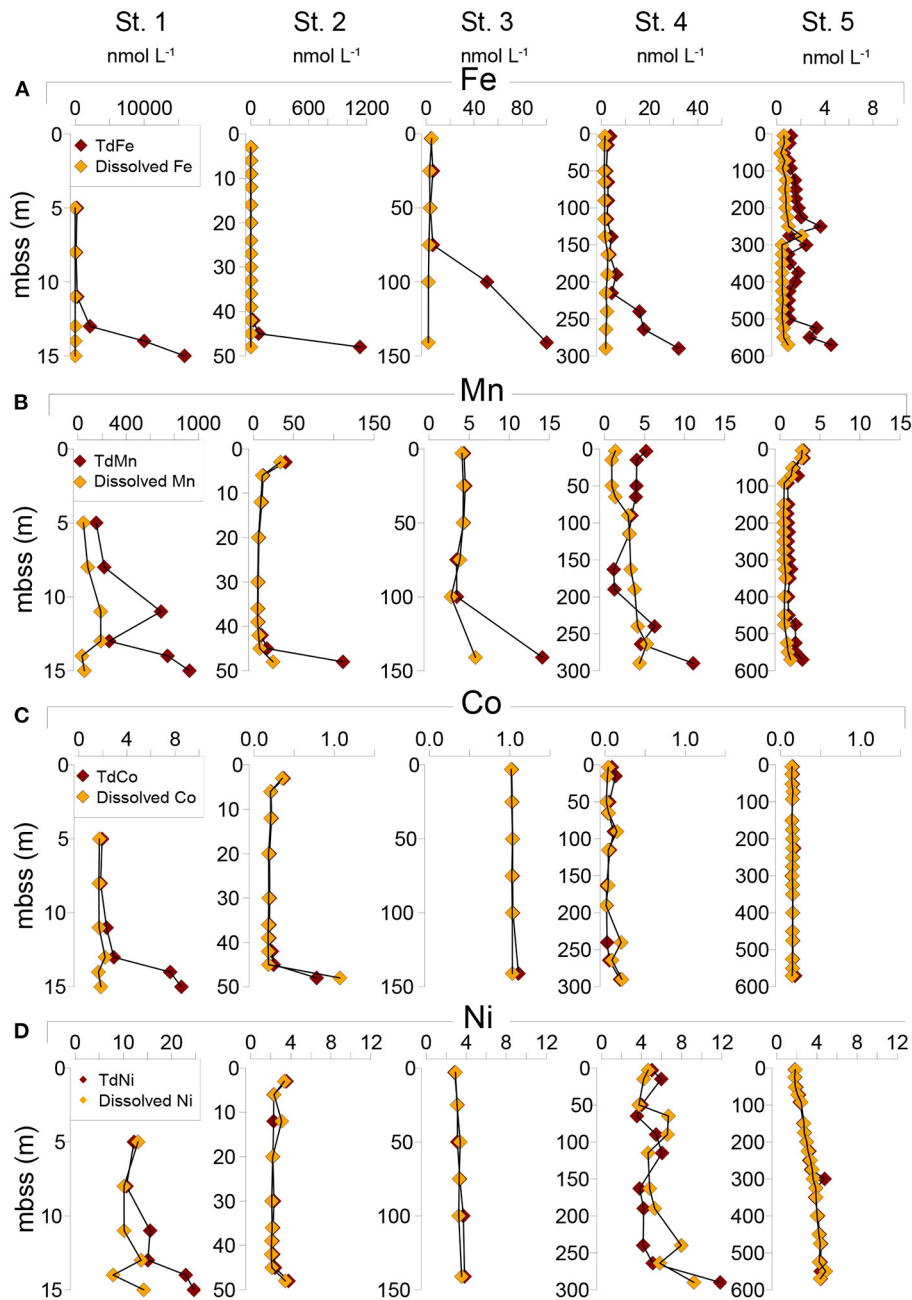


FIGURE 3 | Water column depth profiles in nmol L^{-1} of (A) TdFe and dissolved Fe; (B) TdMn and dissolved Mn; (C) TdCo and dissolved Co and (D) TdNi and dissolved Ni, mbss is meter below sea surface. Note that the water samples at stations 1, 3, and 4 were collected with a regular CTD. This may have led to slightly higher concentrations of dissolved Fe, Co, and Ni, especially at stations 3 and 4. Note the different scales for the x-axes.

contents in the surface sediment varied between 0.5 and 1.3 wt% (Table 2) and little change with depth in the sediment was observed (Supplementary Figure 3).

Porewater profiles of NO_3^- showed a distinct maximum near the sediment-water interface at all stations (Supplementary Figure 4), with the highest penetration depth at the most offshore location (Table 2). Maxima in porewater NO_2^- were observed at the bottom of the NO_3^- -bearing zone.

Below this zone of high NO_2^- , NH_4^+ appeared in the porewater and its concentration increased with depth, especially at the two shelf stations. Porewater SO_4^{2-} showed an opposite trend, with the strongest decrease with depth at the shelf stations and little change at the offshore sites. Concentrations of sulfide were mostly below detection (Supplementary Figure 4). *In-situ* measured rates of oxygen uptake were 17.3 and 23.1 $\text{mmol m}^{-2} \text{d}^{-1}$ for stations 1 and 2, respectively (Table 2). The macrofaunal

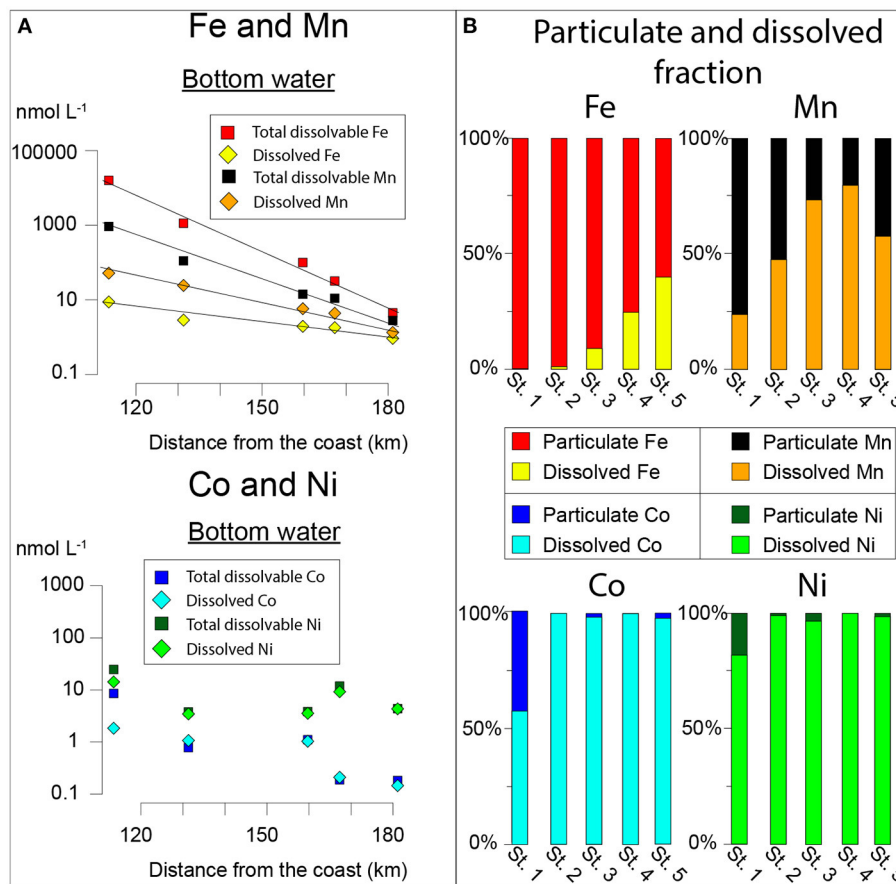


FIGURE 4 | (A): Bottom water concentrations ($nmol L^{-1}$) of total dissolvable and dissolved Fe, Mn, Co, and Ni at station 1 to 5. **(B):** Depth integrated distribution of particulate and dissolved Fe, Mn, Co, and Ni in the water column at stations 1 to 5. The particulate fraction was determined by subtracting the dissolved fraction from the total dissolvable fraction. This particulate fraction is the labile particulate metal fraction. Distance from the coast is defined as the distance to the outflow of the Atchafalaya River (Figure 1).

TABLE 3 | Speciation of Fe for suspended matter collected through *in-situ* filtration at four stations in Fe extraction (Supplementary Table 3).

station	depth m	flow L	Asc. Fe $nmol L^{-1}$	Fe_{ox1} $nmol L^{-1}$	HCl Fe(II) $nmol L^{-1}$	Fe_{ox2} $nmol L^{-1}$	Magnetite $nmol L^{-1}$	Tot. Fe $nmol L^{-1}$
St. 1	1.4	20.0	1.5	2.5	0.9	4.9	0.5	10.3
St. 1	12	300	4.9	7.9	3.3	15.8	1.6	33.5
St. 2	1.5	77.8	0.3	1.7	2.4	4.9	0	9.3
St. 2	51.5	300.0	6.4	19.0	3.0	26.6	2.6	57.6
St. 3	bottom	154.5	2.2	7.7	3.1	0.2	1.6	14.8
St. 5	1.5	78.0	0	0.5	0.4	0	0.6	1.5
St. 5	620	506.0	0.5	0.2	0.1	0.6	0.2	1.6

Asc. Fe is ascorbate acid extractable Fe, HCl Fe(II) (Fe carbonate and FeS), Fe_{ox1} easily reducible Fe oxides, Fe_{ox2} reducible (crystalline) Fe oxides, Fe_{mag} magnetite and total extracted (Tot. Fe) (Supplementary Table 3). The exact sampled depth at station 3 is unknown.

densities for the same stations were 141 and 49 individuals per m^{-2} , respectively (Table 2).

Porewaters at all stations were enriched in dissolved Fe and Mn relative to surface waters, with mostly decreasing concentrations with distance from the coast. At station 1, concentrations of both porewater Fe and Mn were elevated close

to the sediment water interface (ca. 350 and 200 $\mu mol L^{-1}$, respectively; Figure 6A). For Mn, this was also the case at station 2. At all other stations, dissolved Fe and Mn emerged in the porewater only at greater depth in the sediment.

In-situ benthic release of dissolved Fe, Mn, Co, and Ni was highest at station 1 (20, 1760, 2.5, and 1.7 $\mu mol m^{-2} d^{-1}$,

respectively; **Figure 6B** and **Table 4**). At station 2, rates of benthic release of dissolved Fe, Mn, and Co were lower or similar to values at station 1. At stations 1 and 2 the benthic release of DIC was 50 and 30 $mmol\ m^{-2}\ d^{-1}$, respectively (**Table 4**). Calculated diffusive fluxes of dissolved Fe and Mn were high at station 1 and negligible at stations 2-5, except for the calculated diffusive flux of Mn at station 2 (**Table 4**).

Concentrations of easily reducible Fe oxides (Fe_{ox1}) decreased with sediment depth at all stations (**Supplementary Figure 5**). The sediment profiles of Fe_{ox2} , $Fe(II)$, and Fe_{mag} do not show a consistent trend with depth. Concentrations of FeS_x and values of DOP increased with depth at stations 1 and 2 (Fig **Supplementary Figure 3**). At the other stations concentrations of FeS_x were relatively low and constant with depth (**Supplementary Figure 5**). Concentrations of FeS were low at all stations ($<3\ \mu mol\ g^{-1}$). Overall, FeS_x concentrations and DOP values were higher at the two shelf stations 1 and 2 compared to the other stations (**Supplementary Figure 3**).

4. DISCUSSION

4.1. Dynamics of Fe, Mn, Co, and Ni in Continental Shelf and Slope Waters

The Louisiana continental shelf receives large amounts of particulate material from the Mississippi and Atchafalaya Rivers (Trefry et al., 1994; Bianchi et al., 2010). Most of the riverine particles are deposited close to the river mouths, but some fine material remains in suspension and is transported further offshore in buoyant plumes (Wright and Nittrouer, 1995). We find relatively high concentrations of particulate Fe, Mn, Co, and Ni in the turbid waters near the seafloor at our most nearshore station 1 when compared to more offshore parts of the shelf and slope (**Figure 3**). We attribute this to input of river sediments enriched in Fe, Mn, and other trace metals (Shiller and Boyle, 1991; Reiman et al., 2018) supplemented with trace metal-rich particles formed through recycling from the sediment, especially for Mn, Co, and Ni (discussed in section 4.2).

Whether metals in the water column are present in particulate or in dissolved form plays a key role in their transport over continental shelves (Jeandel et al., 2015). The offshore increase in ratios of dissolved Fe/TdFe and dissolved Mn/TdMn in our study area (**Figure 4B**) reveals a more efficient transport of dissolved Fe and Mn compared to particulate Fe and Mn, as

expected (Jeandel et al., 2015). The higher dissolved Mn/TdMn ratio in the water column compared to that for dissolved Fe/TdFe (**Figure 4B**), in turn, points toward more efficient transport of dissolved Mn through the water column when compared to dissolved Fe. More efficient transport of dissolved Mn in shelf waters when compared to Fe was reported previously for the Black Sea shelf (Lenstra et al., 2020). This observation was attributed to faster oxidation kinetics of dissolved Fe when compared to Mn (Thamdrup et al., 1994; Stumm and Morgan, 1996), and differences in organic complexation of dissolved Fe and Mn, with Mn possibly forming stronger complexes (Oldham et al., 2017).

Dissolved Co and Ni in marine waters can be scavenged by Fe and Mn oxides (Goldberg, 1954), or can be incorporated into Mn oxides through co-precipitation induced by Mn oxidizing bacteria (Tebo et al., 1984; Moffett and Ho, 1996). As a consequence, the transport of Co and Ni across continental shelves can be linked to the transport of Fe and Mn oxides (e.g., Little et al., 2015; Vance et al., 2016; Morton et al., 2019). In Louisiana shelf and slope waters, however, Co and Ni is almost solely present in dissolved form, despite the presence of Fe and Mn oxides in the water column (**Figure 4**). The only exception is our most nearshore station, station 1, where particulate Co and Ni was also present, likely because of the riverine input of particulate Co and Ni. We conclude that the offshore transport of Co and Ni in the water column is decoupled from that of particulate Fe and Mn. Such a decoupling could be explained by a low reactivity of Fe and Mn oxides in the water column, hindering binding of Co and Ni. Alternatively, dissolved Co and Ni could be bound to organic ligands in the water column (Saito and Moffett, 2001), thereby preventing scavenging by Fe and Mn oxides. In our case, both factors could contribute, based on two observations. First, we find only very low concentrations of ascorbic-acid extractable Fe and Mn in the suspended matter ($<6.5\ nmol\ L^{-1}$ for Fe, below detection for Mn; **Table 3**) despite high TdFe and TdMn ($15,800$ and $925\ nmol\ L^{-1}$) which is mostly particulate (**Figure 3**). This suggests the abundant presence of less reactive Fe and Mn phases (e.g., clays). Second, waters close to river mouths typically contain high concentrations of organic ligands (Beck et al., 1974; Shiller et al., 2006; Santos-Echeandia et al., 2008). Hence, it is likely that organic complexation prevents scavenging of dissolved Co and Ni by Fe and Mn oxides in the water column.

TABLE 4 | *In-situ* measured benthic fluxes of dissolved Fe, Mn, Co, and Ni and calculated diffusive benthic fluxes of dissolved Fe and Mn.

station	<i>In-situ</i> flux Fe_{diss} $mmol\ m^{-2}\ d^{-1}$	Diffusive flux Fe_{diss} $mmol\ m^{-2}\ d^{-1}$	<i>In-situ</i> flux Mn_{diss} $mmol\ m^{-2}\ d^{-1}$	Diffusive flux Mn_{diss} $mmol\ m^{-2}\ d^{-1}$	<i>In-situ</i> flux Co_{diss} $\mu mol\ m^{-2}\ d^{-1}$	<i>In-situ</i> flux Ni_{diss} $\mu mol\ m^{-2}\ d^{-1}$
St. 1	0.02	1.3	1.8±1.8	2.97	2.5±0.5	1.7±0.2
St. 2	0	-0.002	0.5	0.26	1.7	1.7
St. 3	n.a.	0.004	n.a.	0	n.a.	n.a.
St. 4	n.a.	-0.001	n.a.	-0.004	n.a.	n.a.
St. 5	n.a.	-0.003	n.a.	0	n.a.	n.a.

In-situ measurements are averaged for the number of incubation chambers (**Supplementary Figure 6**); n.a., not available.

4.2. Sediments as a Source and Sink of Trace Metals

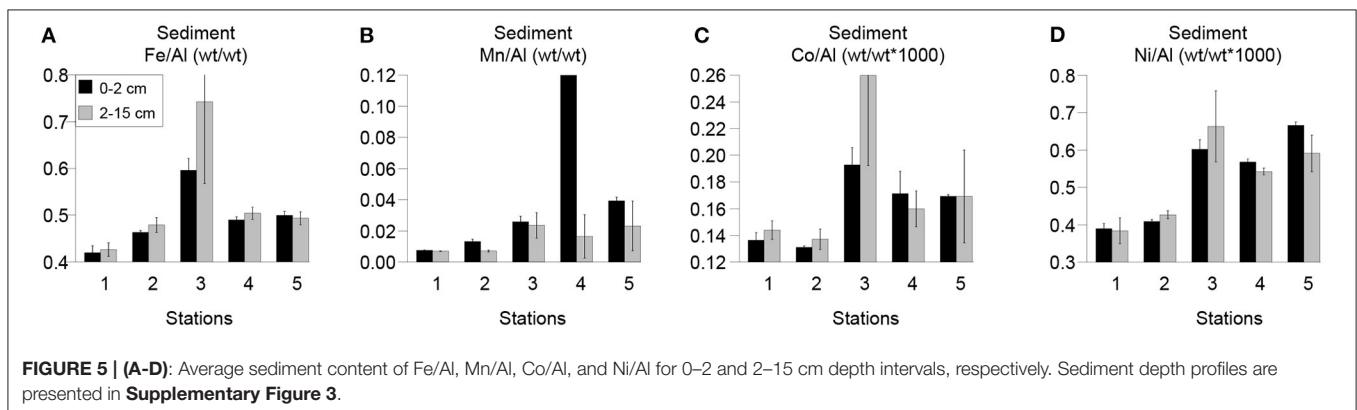
Rates of sediment accumulation and aerobic and anaerobic degradation of organic matter are known to be high in Louisiana shelf sediments near the mouths of the Mississippi/Atchafalaya Rivers (Canfield, 1988; Fennel and Testa, 2019; Owings et al., 2021). At stations 1 and 2, both sedimentation rates ($\sim 1.5 \text{ cm yr}^{-1}$) and rates of benthic oxygen consumption ($17\text{--}26 \text{ mmol m}^{-2} \text{ d}^{-1}$) are indeed high (Table 2). The high oxygen uptake contributes to the hypoxia of the bottom water that typically develops in summer (Fennel and Testa, 2019; Turner and Rabalais, 2019). At the time of sampling in spring 2018 the bottom water oxygen concentration at station 1 was $56 \mu\text{mol L}^{-1}$ and these waters hence qualified as hypoxic (Table 2). At stations 1 and 2, we also observed relatively high rates of anaerobic degradation of organic matter in the sediment, as deduced from the increase in porewater NH_4^+ with depth. At the three more offshore slope stations, in contrast, sedimentation rates are ca. 5 times lower ($0.2\text{--}0.3 \text{ cm yr}^{-1}$) and the shapes of the NH_4^+ profiles point to comparatively low rates of anaerobic degradation of organic matter.

The offshore decline in organic matter input and degradation has profound impacts on the sedimentary cycling of Fe, Mn, Co, and Ni and the potential release of these metals to the water column. For Fe and Mn, this is, especially evident from the porewater profiles that reflect a gradual offshore deepening of the zone of the sediment with elevated porewater concentrations of Fe and Mn (Figure 6). This trend is in accordance with the expected changes in redox zonation in the sediment with lower rates of organic matter input and degradation (e.g., Aller, 2013). At the most nearshore station, station 1, the maxima in porewater Fe and Mn near the sediment-water interface suggest benthic release of dissolved Fe and Mn, as indeed also observed with the *in-situ* chamber incubations (0.02 and $1.8 \text{ mmol m}^{-2} \text{ d}^{-1}$, respectively; Figure 6B). At station 2, the porewater profiles and *in-situ* flux measurements also point toward benthic release of Mn, but not of Fe (Figure 6B). This high benthic release of Mn compared to Fe is in agreement with the much faster oxidation kinetics of Fe^{2+} compared to Mn^{2+} (Thamdrup et al., 1994; Stumm and Morgan, 1996; Ho et al., 2019); while dissolved Mn escapes to the overlying water, most dissolved Fe is retained through oxidation of Fe^{2+} in the oxic surface sediment. At these

stations the macrofaunal densities are relatively low ($<150 \text{ ind. m}^{-2}$) as is typical for hypoxic zones (Levin et al., 2009) and are not expected to play an important role in the benthic release of nutrients and trace metals. At the offshore stations, calculated diffusive fluxes based on porewater data indicate that benthic release of Fe and Mn is unlikely (Figure 6A and Table 4).

Unfortunately, porewater profiles of Co and Ni are not available for these stations, because concentrations were below the detection limit. However, the lander incubations reveal substantial release of Co and Ni from the sediment to the overlying water at both shelf stations (St.1: 2.5 and $1.7 \mu\text{mol m}^{-2} \text{ d}^{-1}$ and St.2: 1.7 and $1.7 \mu\text{mol m}^{-2} \text{ d}^{-1}$, respectively; Figure 6). Cobalt and Ni are known to have a high affinity to Mn oxides (Moffett and Ho, 1996; Peacock and Sherman, 2007) and Mn oxide reduction may be responsible for the release of Co and Ni at these stations (Figure 6). Given the much lower rates of input and degradation of organic matter and lack of Fe and Mn oxide reduction near the sediment-water interface at the slope stations, only little production of Co and Ni in the porewater and benthic release of these trace metals is expected in this region.

We note that our benthic flux and porewater sampling only captured the situation in spring prior to the onset of widespread hypoxia on the shelf. At lower bottom water oxygen concentrations, as typically occur in the region in summer (Rabalais et al., 2007; Devereux et al., 2015; Pitcher et al., 2021), benthic release of the trace metals is expected to be enhanced because of lower rates of metal oxidation with oxygen (e.g., Sundby et al., 1986; Severmann et al., 2010). The strongest seasonal contrast is expected for Fe. While Fe is efficiently retained in the sediment in spring (Table 2), the Fe is expected to escape to the overlying water when bottom waters are low in oxygen and sulfide is absent from the porewater later in the year, as is observed in other systems (Severmann et al., 2010; Dale et al., 2015). The potential for benthic release of Fe from Louisiana shelf sediments upon the onset of hypoxia was illustrated previously through incubation experiments of sediment cores (Ghaisas et al., 2019). In these experiments, benthic Fe fluxes reached a maximum of $0.45 \text{ mmol m}^{-2} \text{ d}^{-1}$, a value which falls within the range of benthic Fe fluxes observed for other river-dominated continental shelves, such as the California-Oregon shelf and northwestern Black Sea shelf (between 0.012 and $0.57 \text{ mmol m}^{-2} \text{ d}^{-1}$; Severmann et al., 2010; Lenstra et al., 2019).



Sediment trace metal contents normalized to Al can provide further insight into the role of the seafloor as a source and sink of trace metals (e.g., Lyons and Severmann, 2006; Scholz et al., 2014; Plass et al., 2021). In such calculations, low values relative to Al are indicative of a trace metal source whereas high values represent a sink. We find very low ratios of Fe/Al, Mn/Al, Co/Al, and Ni/Al at the shelf stations 1 and 2 compared to the slope stations 3–5. This confirms that these shelf sediments act as a source of trace metals to the water column, in accordance with the trends in the porewater profiles of Fe and Mn and measured *in-situ* benthic release (Figure 6). The slope sediments, in turn, are enriched in trace metals, suggesting that they act as a sink (Figures 5, 7). Such an offshore trend in sediment metal content was previously observed for Fe and Mn on the continental shelf of the northwestern Black Sea (Lenstra et al., 2019, 2020) and in the Gulf of California (Scholz et al., 2019). This implies that the supply of dissolved trace metals from continental shelves to the open ocean may, in many cases, depend on sediment processes in nearshore areas where organic matter input is relatively high.

Escape of trace metals from sediments to the water column is typically thought to be most pronounced under oxygen-depleted but non-sulfidic bottom water conditions (Scholz et al., 2014). In Louisiana shelf sediments, DOP values and pyrite content were higher at the shelf stations 1 and 2 when compared to the slope stations (Supplementary Figure 3). This reflects the higher rates of organic matter input and associated sulfate reduction at the shelf locations. Importantly, however, easily reducible Fe oxides were also present in the sediment down to a depth of at least 15 cm (Supplementary Figure 5), sediment FeS concentrations were low and sulfide was absent from the porewater at these stations (Supplementary Figures 4, 5). This is in accordance with previous work for this region showing that the high riverine input of reactive Fe allows the porewaters and bottom waters to remain sulfide-free (e.g., Canfield, 1988). Hence, retention of metals in sulfides in the sediment is expected to play a minor role only.

4.3. Implications

Continental shelves are an important source of trace metals to the open ocean (e.g., Lam and Bishop, 2008; Lam et al., 2012; Noble et al., 2017). The trace metals can be transported laterally in the water column in both particulate and dissolved form. On river-dominated shelves, the trace metals may directly originate from riverine input but may also be subject to recycling between the water column and sediment (Figure 7). On the section of the Louisiana shelf and slope studied here, substantial benthic release of Fe, Mn, Co, and Ni occurs in the nearshore shelf region affected by seasonal hypoxia. In this shelf area the input of organic matter is sufficiently high to drive the mobilization and benthic release of trace metals from the sediment (Figure 6B). Because Fe oxides are abundant, porewater sulfide concentrations remain low and sulfidization of Fe (Supplementary Figure 3), Mn (Lenstra et al., 2021a) and likely also of Co and Ni is limited. Our work confirms earlier studies that Mn is more mobile on continental shelves than Fe (Thamdrup et al., 1994; Lenstra et al., 2020). In the slope sediments (stations 3–5) the input of organic matter is lower and the sediments act as a sink for incoming Fe, Mn, Co,

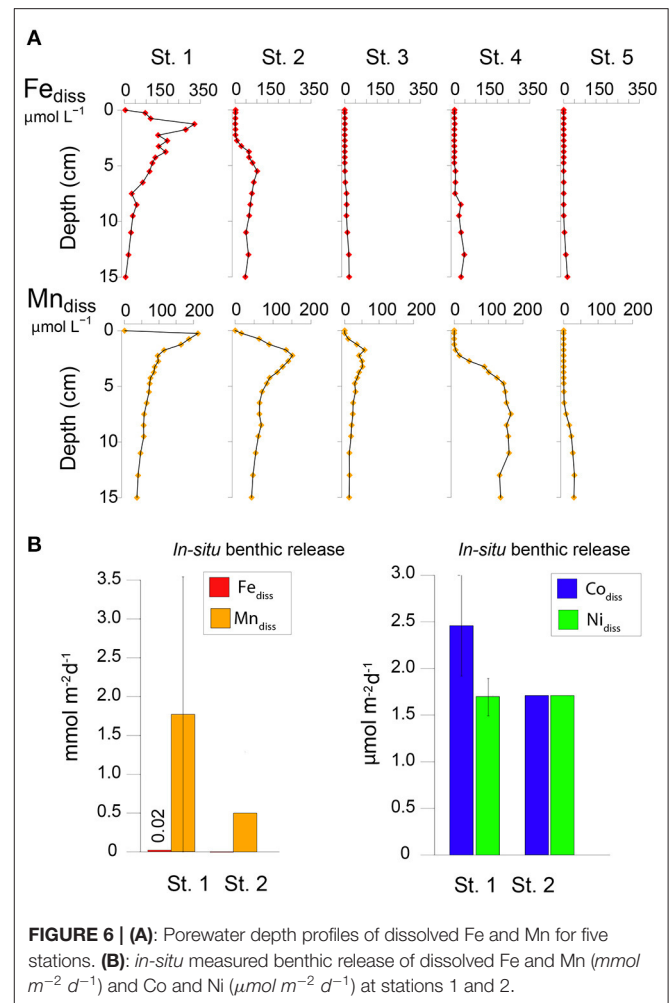


FIGURE 6 | (A): Porewater depth profiles of dissolved Fe and Mn for five stations. **(B):** *in-situ* measured benthic release of dissolved Fe and Mn ($\text{mmol m}^{-2} \text{d}^{-1}$) and Co and Ni ($\mu\text{mol m}^{-2} \text{d}^{-1}$) at stations 1 and 2.

and Ni, with most metals likely bound to sedimentary oxides. This spatial contrast highlights the combined role of organic matter input, the presence of reactive Fe oxides and bottom water oxygen in determining trace metal release from and retention in sediments of continental margins. Our results also highlight that, on river-dominated shelves, a relatively small area in the vicinity of river mouths likely accounts for most release of metals from the sediment to the water column.

While most water column Fe and Mn is present in particulate form close to the seafloor, Co and Ni are nearly exclusively present in dissolved form (Figures 4, 7). This decoupling has important implications for the transport of these metals, since dissolved forms will travel further, as is also evident from the offshore increase in dissolved/total dissolvable Fe, Mn, Co, and Ni (Figure 4B). A decoupling of water column transport of Fe and Mn versus Co and Ni was observed previously in waters of the Bering Strait (Vieira et al., 2019), and for Mn and Co, in offshore waters of the Western North Pacific (Morton et al., 2019). Our findings imply that the role of Fe and Mn oxides in the transport of Co and Ni over continental shelves might be less important than previously thought (Little et al., 2015;

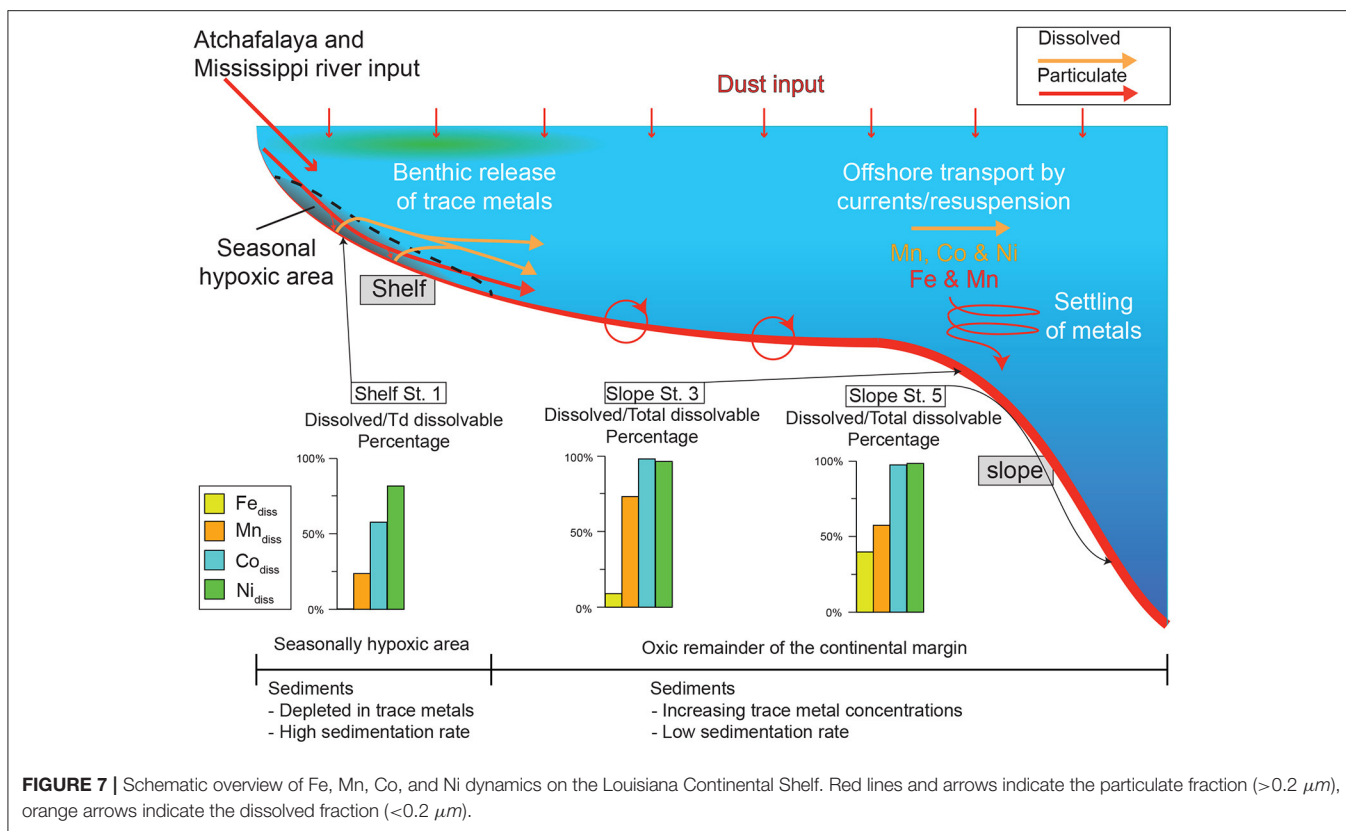


FIGURE 7 | Schematic overview of Fe, Mn, Co, and Ni dynamics on the Louisiana Continental Shelf. Red lines and arrows indicate the particulate fraction ($>0.2 \mu\text{m}$), orange arrows indicate the dissolved fraction ($<0.2 \mu\text{m}$).

Vance et al., 2016). We suggest that the decoupling may be due to differences in complexation with organic ligands and/or the crystallinity and hence reactivity of the Fe and Mn oxides. Further work is needed to elucidate the exact mechanisms for the decoupling of the water column transport of Fe and Mn versus Co and Ni.

DATA AVAILABILITY STATEMENT

The original contributions presented in the study are included in the article/**Supplementary Material**, further inquiries can be directed to the corresponding author/s.

AUTHOR CONTRIBUTIONS

WL and CS designed the research and wrote the paper with comments provided by NH. WL, NH, OŽ, RZ, and RW performed the geochemical sampling and analyses. WL, NH, and CS interpreted the data. All authors contributed to the article and approved the submitted version.

REFERENCES

- Aller, R. C. (2013). Sedimentary diagenesis, depositional environments, and benthic fluxes. *Treatise Geochem.* *Second Ed.*, 8, 293–334. doi: 10.1016/B978-0-08-095975-7.00611-2
- Beck, K. C., Reuter, J. H., and Perdue, E. M. (1974). Organic and inorganic geochemistry of some coastal plain rivers of the southeastern

FUNDING

This research was funded by NWO-Vici grant 865.13.005 (to CS) and ERC Synergy project MARIX (8540088). This work was carried out under the program of the Netherlands Earth System Science Centre (NESSC), financially supported by the Ministry of Education, Culture and Science (OCW).

ACKNOWLEDGMENTS

We thank the captain, crew, technicians, (co-)chief scientists D. Rush and Z. Erdem and all other scientists aboard R/V Pelagia during cruise 64PE434 of the Netherlands Initiative Changing Oceans Program (NICO) in March 2018, for their assistance. We also thank H. de Waard, C. Mulder, M. Séguret, and A. van Dijk for analytical assistance in Utrecht.

SUPPLEMENTARY MATERIAL

The Supplementary Material for this article can be found online at: <https://www.frontiersin.org/articles/10.3389/fmars.2022.811953/full#supplementary-material>

- United States. *Geochimica et Cosmochimica Acta* 38, 341–364. doi: 10.1016/0016-7037(74)90130-6
- Bianchi, T. S., DiMarco, S. F., Cowan Jr, J. H., Hetland, R. D., Chapman, P., Day, J. W., et al. (2010). The science of hypoxia in the Northern Gulf of Mexico: a review. *Sci. Total Environ.*, 408(7):1471–1484. doi: 10.1016/j.scitotenv.2009.11.047
- Brewer, P. G., and Spencer, D. W. (1971). Colorimetric determination of manganese in anoxic waters. *Limnol. Oceanography* 16, 107–110. doi: 10.4319/lo.1971.16.1.0107
- Burdige, D. J. (2006). *Geochemistry of Marine Sediments*. Princeton University Press.
- Burton, E. D., Sullivan, L. A., Bush, R. T., Johnston, S. G., and Keene, A. F. (2008). A simple and inexpensive chromium-reducible sulfur method for acid-sulfate soils. *Appl. Geochem.* 23, 2759–2766. doi: 10.1016/j.apgeochem.2008.07.007
- Canfield, D. E. (1988). Reactive iron in marine sediments. *Geochimica et Cosmochimica Acta* 53, 619–632. doi: 10.1016/0016-7037(89)90005-7
- Charette, M. A., Lam, P. J., Lohan, M. C., Kwon, E. Y., Hatje, V., Jeandel, C., et al. (2016). Coastal ocean and shelf-sea biogeochemical cycling of trace elements and isotopes: lessons learned from GEOTRACES. *Philosoph. Trans. R. Soc.* 374:20160076. doi: 10.1098/rsta.2016.0076
- Claff, S. R., Sullivan, L. A., Burton, E. D., and Bush, R. T. (2010). A sequential extraction procedure for acid sulfate soils: Partitioning of iron. *Geoderma* 155, 224–230. doi: 10.1016/j.geoderma.2009.12.002
- Cline, J. D. (1969). Spectrophotometric determination of hydrogen sulfide in natural waters. *Limnol. Oceanography* 14, 454–458. doi: 10.4319/lo.1969.14.3.0454
- Dale, A. W., Nickelsen, L., Scholz, F., Hensen, C., Oschlies, A., and Wallmann, K. (2015). A revised global estimate of dissolved iron fluxes from marine sediments. *Glob. Biogeochem. Cycles* 29, 691–707. doi: 10.1002/2014GB005017
- Devereux, R., Lehrter, J. C., Beddick, D. L., Yates, D. F., and Jarvis, B. M. (2015). Manganese, iron, and sulfur cycling in Louisiana continental shelf sediments. *Continental Shelf Research* 17, 46–56. doi: 10.1016/j.csr.2015.03.008
- Eleftheriou, A., and McIntyre, A. (2007). *Methods for the Study of Marine Benthos: Third Edition*. Blackwell Publishin Ltd.
- Federation, Water Environmental, and APH Association (2005). *Standard Methods for the Examination of Water and Wastewater*. Washington, DC: American Public Health Association (APHA).
- Fennel, K., and Testa, J. M. (2019). Annual review of marine science biogeochemical controls on coastal hypoxia. *Ann. Rev. Marine Sci.* 11, 105–130. doi: 10.1146/annurev-marine-010318-095138
- Ghaisas, N. A., Maiti, K., and White, J. R. (2019). Coupled iron and phosphorus release from seasonally hypoxic Louisiana shelf sediment. *Estuarine Coastal Shelf Sci.* 219, 81–89. doi: 10.1016/j.ecss.2019.01.019
- Gledhill, M., and van den Berg, C. M. G. (1994). Determination of complexation of iron(III) with natural organic complexing ligands in seawater using cathodic stripping voltammetry. *Marine Chem.* 47, 41–54. doi: 10.1016/0304-4203(94)90012-4
- Goldberg, E. D. (1954). Marine geochemistry I. Chemical scavengers of the sea. *J. Geol.* 62, 249–265.
- Grasshoff, K., and Ehrhardt, M. (1983). Automated chemical analysis. *Methods of Seawater Analysis*. (Verlag), 263–289.
- Henderson, G. M., Achterberg, E. P., and Bopp, L. (2018). Changing trace element cycles in the 21st century ocean. *Elements Int. Mag. Mineral. Geochem. Petrol.* 14, 409–413. doi: 10.2138/gselements.14.6.409
- Ho, P., Shim, M. J., Howden, S. D., and Shiller, A. M. (2019). Temporal and spatial distributions of nutrients and trace elements (Ba, Cs, Cr, Fe, Mn, Mo, U, V and Re) in Mississippi coastal waters: influence of hypoxia, submarine groundwater discharge, and episodic events. *Continental Shelf Res.* 175, 53–69. doi: 10.1016/j.csr.2019.01.013
- Huerta-Diaz, M. A., and Morse, J. W. (1992). Pyritization of trace metals in anoxic marine sediments. *Geochimica et Cosmochimica Acta* 56, 2681–2702. doi: 10.1016/0016-7037(92)90353-K
- Jeandel, C., van Der Loeff, M. R., Lam, P. J., Roy-Barman, M., Sherrell, R. M., Kretschmer, S., et al. (2015). What did we learn about ocean particle dynamics in the GEOSECS JGOFS era? *Progr. Oceanography* 133, 6–16. doi: 10.1016/j.pocean.2014.12.018
- Klar, J. K., Homoky, W. B., Statham, P. J., Birchill, A. J., Harris, E. L., Woodward, E. M. S., et al. (2017). Stability of dissolved and soluble Fe(II) in shelf sediment pore waters and release to an oxic water column. *Biogeochemistry* 135, 49–67. doi: 10.1007/s10533-017-0309-x
- Klunder, M. B., Laan, P., Middag, R., De Baar, H. J. W., and van Ooijen, J. C. (2011). Dissolved iron in the Southern Ocean (Atlantic sector). *Deep-Sea Res. Part II Top. Stud. Oceanography* 58, 2678–2694. doi: 10.1016/j.dsr2.2010.10.042
- Koroleff, F. (1969). "Direct determination of ammonia in natural waters as indophenol blue," in *ICES, CM*, Vol. 100, 9.
- Kraal, P., Slomp, C. P., Forster, A., Kuypers, M. M. M., and Sluifs, A. (2009). Pyrite oxidation during sample storage determines phosphorus fractionation in carbonate-poor anoxic sediments. *Geochimica et Cosmochimica Acta* 73, 3277–3290. doi: 10.1016/j.gca.2009.02.026
- Lam, P. J., and Bishop, J. K. B. (2008). The continental margin is a key source of iron to the HNLC North Pacific Ocean. *Geophys. Res. Lett.* 35, L07608. doi: 10.1029/2008GL033294
- Lam, P. J., Ohnemus, D. C., and Marcus, M. A. (2012). The speciation of marine particulate iron adjacent to active and passive continental margins. *Geochimica et Cosmochimica Acta* 80, 108–124. doi: 10.1016/j.gca.2011.11.044
- Large, R. R., Halpin, J. A., Danyushevsky, L. V., Maslennikov, V. V., Bull, S. W., Long, J. A., et al. (2014). Trace element content of sedimentary pyrite as a new proxy for deep-time ocean-atmosphere evolution. *Earth Planetary Sci. Lett.* 389, 209–220. doi: 10.1016/j.epsl.2013.12.020
- Lenstra, W. K., Hermans, M., Séguret, M. J., Witbaard, R., Behrends, T., Dijkstra, N., et al. (2019). The shelf-to-basin iron shuttle in the Black Sea revisited. *Chem. Geol.* 511, 314–341. doi: 10.1016/j.chemgeo.2018.10.024
- Lenstra, W. K., Hermans, M., Séguret, M. J. M., Witbaard, R., Severmann, S., Behrends, T., and Slomp, C. P. (2021a). Coastal hypoxia and eutrophication as key controls on benthic release and water column dynamics of iron and manganese. *Limnol. Oceanography* 66, 807–826. doi: 10.1002/lno.11644
- Lenstra, W. K., Klomp, R., Molema, F., Behrends, T., and Slomp, C. P. (2021b). A sequential extraction procedure for particulate manganese and its application to coastal marine sediments. *Chem. Geol.* 584:120538. doi: 10.1016/j.chemgeo.2021.120538
- Lenstra, W. K., Séguret, M. J. M., Behrends, T., Groeneveld, R. K., Hermans, M., Witbaard, R., et al. (2020). Controls on the shuttling of manganese over the northwestern Black Sea shelf and its fate in the euxinic deep basin. *Geochimica et Cosmochimica Acta* 273, 177–204.
- Levin, L. A., Ekau, W., Gooday, A. J., Jorissen, F., Middelburg, J. J., Naqvi, S. W. A., et al. (2009). Effects of natural and human-induced hypoxia on coastal benthos. *Biogeosciences* 6, 2063–2098. doi: 10.5194/bg-6-2063-2009
- Little, S. H., Vance, D., Lyons, T. W., and McManus, J. (2015). Controls on trace metal authigenic enrichment in reducing sediments: insights from modern oxygen-deficient settings. *Am. J. Sci.* 315, 77–119. doi: 10.2475/02.2015.01
- Lyons, T. W., and Severmann, S. (2006). A critical look at iron paleoredox proxies: new insights from modern euxinic marine basins. *Geochimica et Cosmochimica Acta* 70, 5698–5722. doi: 10.1016/j.gca.2006.08.021
- McManus, J., Berelson, W. M., Severmann, S., Johnson, K. S., Hammond, D. E., Roy, M., et al. (2012). Benthic manganese fluxes along the Oregon-California continental shelf and slope. *Continental Shelf Res.* 43, 71–85. doi: 10.1016/j.csr.2012.04.016
- Mellet, T., and Busck, K. N. (2020). Spatial and temporal variability of trace metals (Fe, Cu, Mn, Zn, Co, Ni, Cd, Pb), iron and copper speciation, and electroactive Fe-binding humic substances in surface waters of the eastern Gulf of Mexico. *Marine Chem.* 227:103891.
- Meaybeck, M. (2003). Global analysis of river systems: From Earth system controls to Anthropocene syndromes. *Philosoph. Trans. R. Soc. B Biol. Sci* 358, 1935–1955. doi: 10.1098/rstb.2003.1379
- Moffett, J. W., and Ho, J. (1996). Oxidation of cobalt and manganese in seawater via a common microbially catalyzed pathway. *Geochimica et Cosmochimica Acta* 60, 3415–3424. doi: 10.1016/0016-7037(96)00176-7
- Morton, P. L., Landing, W. M., Shiller, A. M., Moody, A., Kelly, T. D., Bizimis, M., et al. (2019). Shelf Inputs and Lateral Transport of Mn, Co, and Ce in the Western North Pacific Ocean. *Front. Marine Sci.* 6:591. doi: 10.3389/fmars.2019.00591
- Noble, A. E., Ohnemus, D. C., Hawco, N. J., Lam, P. J., and Saito, M. A. (2017). Coastal sources, sinks and strong organic complexation of dissolved cobalt

- within the US North Atlantic GEOTRACES transect GA03. *Biogeoscience* 14, 2715–2739. doi: 10.5194/bg-14-2715-2017
- Oldham, V. E., Mucci, A., Tebo, B. M., and Luther, G. W. (2017). Soluble Mn(III)L complexes are abundant in oxygenated waters and stabilized by humic ligands. *Geochimica et Cosmochimica Acta* 199, 238–246. doi: 10.1016/j.gca.2016.11.043
- Owings, S. M., Bréthous, L., Eitel, E. M., Fields, B. P., Boever, A., Beckler, J. S., et al. (2021). Differential manganese and iron recycling and transport in continental margin sediments of the Northern Gulf of Mexico. *Marine Chem.* 229:103908. doi: 10.1016/j.marchem.2020.103908
- Peacock, C. L., and Sherman, D. M. (2007). Sorption of Ni by birnessite: Equilibrium controls on Ni in seawater. *Chem. Geol.* 238, 94–106. doi: 10.1016/j.chemgeo.2006.10.019
- Pitcher, G. C., Aguirre-Velarde, A., Breitburg, D., Cardich, J., Carstensen, J., Conley, D. J., et al. (2021). System controls of coastal and open ocean oxygen depletion. *Progr. Oceanography*. 197: 102613. doi: 10.1016/j.pocean.2021.102613
- Plass, A., Dale, A. W., and Scholz, F. (2021). Sedimentary cycling and benthic fluxes of manganese, cobalt, nickel, copper, zinc and cadmium in the Peruvian oxygen minimum zone. *Marine Chem.* 233:103982. doi: 10.1016/j.marchem.2021.103982
- Rabalais, N. N., Turner, R. E., Gupta, B. K. S., Boesch, D. F., Chapman, P., and Murrell, M. C. (2007). Hypoxia in the northern Gulf of Mexico: does the science support the plan to reduce, mitigate, and control hypoxia? *Estuaries Coasts* 30, 753–772. doi: 10.1007/BF02841332
- Rabalais, N. N., Turner, R. E., and Wiseman, W. J. (2002). Gulf of Mexico Hypoxia, A.K.A. “The Dead Zone”. *Ann. Rev. Ecol. Systematics* 33, 235–263. doi: 10.1146/annurev.ecolsys.33.010802.150513
- Raiswell, R., and Canfield, D. E. (2012). The iron biogeochemical cycle past and present. *Geochim. Perspectives* 1, 1–220. doi: 10.7185/geochemsp.1.1
- Raiswell, R., Vu, H. P., Brinza, L., and Benning, L. G. (2010). The determination of labile Fe in ferrihydrite by ascorbic acid extraction: Methodology, dissolution kinetics and loss of solubility with age and de-watering. *Chem. Geol.* 278, 70–79. doi: 10.1016/j.chemgeo.2010.09.002
- Reiman, J. H., Xu, Y. J., He, S., and DelDuco, E. M. (2018). Metals geochemistry and mass export from the Mississippi-Atchafalaya River system to the Northern Gulf of Mexico. *Chemosphere* 205, 559–569. doi: 10.1016/j.chemosphere.2018.04.094
- Rijkenberg, M. J. A., de Baar, H. J. W., Bakker, K., Gerringa, L. J. A., Keijzer, E., Laan, M., Laan, et al. (2015). “PRISTINE”, a new high volume sampler for ultraclean sampling of trace metals and isotopes. *Marine Chem.* 177, 501–509. doi: 10.1016/j.marchem.2015.07.001
- Saito, M. A., and Moffett, J. W. (2001). Complexation of cobalt by natural organic ligands in the Sargasso sea as determined by a new high-sensitivity electrochemical cobalt speciation method suitable for open ocean work. *Marine Chem.* 75, 49–68. doi: 10.1016/S0304-4203(01)00025-1
- Santos-Echeandia, J., Laglera, L. M., Prego, R., and van den Berg, C. M. G. (2008). Dissolved copper speciation behaviour during estuarine mixing in the San Simon Inlet (wet season, Galicia). Influence of particulate matter. *Estuarine Coastal Shelf Sci.* 76, 447–453. doi: 10.1016/j.ecss.2007.07.007
- Santos-Echeandia, J., Prego, R., Cobelo-García, A., and Millward, G. E. (2009). Porewater geochemistry in a Galician Ria (NW Iberian Peninsula): implications for benthic fluxes of dissolved trace elements (Co, Cu, Ni, Pb, V, Zn). *Marine Chem.* 117, 77–87. doi: 10.1016/j.marchem.2009.05.001
- Schlitzer, R. (2015). *Ocean Data View*. 2012. Available online at: <http://odv.awi.de>.
- Scholz, F., McManus, J., Mix, A. C., Hensen, C., and Schneider, R. R. (2014). The impact of ocean deoxygenation on iron release from continental margin sediments. *Nat. Geosci.* 7, 433–437. doi: 10.1038/ngeo2162
- Scholz, F., Schmidt, M., Hensen, C., Eroglu, S., Geilert, S., Gutjahr, M., et al. (2019). Shelf-to-basin iron shuttle in the Guaymas Basin, Gulf of California. *Geochimica et Cosmochimica Acta* 261, 76–92. doi: 10.1016/j.gca.2019.07.006
- Severmann, S., McManus, J., Berelson, W. M., and Hammond, D. E. (2010). The continental shelf benthic iron flux and its isotope composition. *Geochimica et Cosmochimica Acta* 74, 3984–4004. doi: 10.1016/j.gca.2010.04.022
- Shiller, A. M. and Boyle, E. A. (1991). Trace elements in the Mississippi River Delta outflow region: behavior at high discharge. *Geochimica et Cosmochimica Acta* 55, 3241–3251. doi: 10.1016/0016-7037(91)90486-O
- Shiller, A. M., Duan, S., Van Erp, P., and Bianchi, T. S. (2006). Photo-oxidation of dissolved organic matter in river water and its effect on trace element speciation. *Limnol. Oceanography* 51, 1716–1728. doi: 10.4319/lo.2006.51.4.1716
- Slomp, C., Malschaert, J., Lohse, L., and Van Raaphorst, W. (1997). Iron and manganese cycling in different sedimentary environments on the North Sea continental margin. *Continental Shelf Res.* 17, 1083–1117. doi: 10.1016/S0278-4343(97)00005-8
- Soetaert, K., Petzoldt, T., and Meysman, F. J. R. (2010). Marelac: tools for aquatic sciences v2.1.3. *R Package*.
- Stumm, W., and Morgan, J. J. (1996). *Aquatic Chemistry: Chemical Equilibria and Rates in Natural Waters*. John Wiley & Sons.
- Sundby, B., Anderson, L. G., Hall, P. O. J., Iverfeldt, Å., van der Loeff, M. M. R., and Westerlund, S. F. G. (1986). The effect of oxygen on release and uptake of cobalt, manganese, iron and phosphate at the sediment-water interface. *Geochimica et Cosmochimica Acta* 50, 1281–1288.
- Tebo, B. M., Neelson, K. H., Emerson, S., and Jacobs, L. (1984). Microbial mediation of Mn(II) and Co(II) precipitation at the O₂/H₂S interfaces in two anoxic fjords. *Limnol. Oceanography* 29, 1247–1258. doi: 10.4319/lo.1984.29.6.1247
- Thamdrup, B., Fossing, H., and Jørgensen, B. B. (1994). Manganese, iron and sulfur cycling in a coastal marine sediment, Aarhus bay, Denmark. *Geochimica et Cosmochimica Acta* 58, 5115–5129. doi: 10.1016/0016-7037(94)90298-4
- Trefry, J. H., Metz, S., Nelsen, T. A., Trocine, R. P., and Eadie, B. J. (1994). Transport of particulate organic carbon by the Mississippi River and its fate in the Gulf of Mexico. *Estuaries* 17, 839. doi: 10.2307/1352752
- Tribouillard, N., Algeo, T. J., Lyons, T., and Riboulleau, A. (2006). Trace metals as paleoredox and paleoproductivity proxies: an update. *Chem. Geol.* 232, 12–32. doi: 10.1016/j.chemgeo.2006.02.012
- Turner, R. E., and Rabalais, N. N. (2019). “The Gulf of Mexico,” in *World Seas: An Environmental Evaluation* (Elsevier), 445–464.
- Van Santvoort, P. J., De Lange, G. J., Thomson, J., Colley, S., Meysman, F. J., and Slomp, C. P. (2002). Oxidation and origin of organic matter in surficial Eastern Mediterranean hemipelagic sediments. *Aquatic Geochem.* 8, 153–175. doi: 10.1023/A:1024271706896
- Vance, D., Little, S. H., Archer, C., Cameron, V., Andersen, M. B., Rijkenberg, M. J., et al. (2016). The oceanic budgets of nickel and zinc isotopes: The importance of sulfidic environments as illustrated by the Black Sea. *Philosoph. Trans. R. Soc. A Math. Phys. Eng. Sci.* 374:20150294. doi: 10.1098/rsta.2015.0294
- Vieira, L. H., Achterberg, E. P., Scholten, J., Beck, A. J., Liebetrau, V., Mills, M. M., et al. (2019). Benthic fluxes of trace metals in the Chukchi Sea and their transport into the Arctic Ocean. *Marine Chem.* 208, 43–55. doi: 10.1016/j.marchem.2018.11.001
- Wells, J. T., and Kim, S.-Y. (1991). The relationship between beam transmission and concentration of suspended particulate material in the Neuse River estuary, North Carolina. *Estuaries* 14, 395–403. doi: 10.2307/1352264
- Witbaard, R., Duineveld, G. C. A., Van der Weele, J. A., Berghuis, E. M., and Reyss, J. P. (2000). The benthic response to the seasonal deposition of phytopigments at the Porcupine Abyssal Plain in the North East Atlantic. *J. Sea Res.* 43, 15–31. doi: 10.1016/S1385-1101(99)00040-4
- Wright, L. D., and Nittrouer, C. A. (1995). Dispersal of river sediments in coastal seas: six contrasting cases. *Estuaries* 18, 494–508. doi: 10.2307/1352367

Conflict of Interest: The authors declare that the research was conducted in the absence of any commercial or financial relationships that could be construed as a potential conflict of interest.

Publisher’s Note: All claims expressed in this article are solely those of the authors and do not necessarily represent those of their affiliated organizations, or those of the publisher, the editors and the reviewers. Any product that may be evaluated in this article, or claim that may be made by its manufacturer, is not guaranteed or endorsed by the publisher.

Copyright © 2022 Lenstra, van Helmond, Żygadłowska, van Zummeren, Witbaard and Slomp. This is an open-access article distributed under the terms of the Creative Commons Attribution License (CC BY). The use, distribution or reproduction in other forums is permitted, provided the original author(s) and the copyright owner(s) are credited and that the original publication in this journal is cited, in accordance with accepted academic practice. No use, distribution or reproduction is permitted which does not comply with these terms.